Stem Cell Research (2013) 10, 133–146

Available online at www.sciencedirect.com

SciVerse ScienceDirect

www.elsevier.com/locate/scr

METHODS AND REAGENTS

Efficient neuronal *in vitro* and *in vivo* differentiation after immunomagnetic purification of mESC derived neuronal precursors

Serena Barral [a, 1], Josephine Ecklebe [a], Stefan Tomiuk [a], Marie-Catherine Tiveron [b, 2], Angélique Desoeuvre [b, 3], Dominik Eckardt [a], Harold Cremer [b, 4], Andreas Bosio [a,*]

[a] *Miltenyi Biotec GmbH, 51429 Bergisch Gladbach, Germany*
[b] *Institut de Biologie du Développement de Marseille-Luminy, Unité Mixte de Recherche 6216, Centre National de la Recherche Scientifique/Université de la Méditerranée, Campus de Luminy, 13288 Marseille, France*

Received 26 April 2012; received in revised form 22 October 2012; accepted 25 October 2012
Available online 2 November 2012

Abstract The cellular heterogeneity that is generated during the differentiation of pluripotent stem cells into specific neural subpopulations represents a major obstacle for experimental and clinical progress. To address this problem we developed an optimized strategy for magnetic isolation of PSA-NCAM positive neuronal precursors from embryonic stem cells (ESCs) derived neuronal cultures. PSA-NCAM enrichment at an early step of the *in vitro* differentiation process increased the number of ES cell derived neurons and reduced cellular diversity. Gene expression analysis revealed that mainly genes involved in neuronal activity were over-represented after purification. *In vitro* derived PSA-NCAM$^+$ enriched precursors were characterized *in vivo* through grafting into the forebrain of adult mice. While unsorted control cells 40 days post graft gave rise to a mixed population composed of immature precursors, early postmitotic neurons and glial cells, PSA-NCAM$^+$ enriched cells differentiated predominantly into NeuN positive cells. Furthermore, PSA-NCAM enriched population showed efficient migration towards the olfactory bulb after transplantation into the rostral migratory stream of the forebrain neurogenic system. Thus,

* Corresponding author.
E-mail addresses: serena.barral@univ-amu.fr, serenab@external.miltenyibiotec.de (S. Barral), JosephineE@miltenyibiotec.de (J. Ecklebe), StefanT@miltenyibiotec.de (S. Tomiuk), marie-catherine.tiveron@univ-amu.fr (M.-C. Tiveron), angelique.desoeuvre@msem.univ-montp2.fr (A. Desoeuvre), dominike@miltenyibiotec.de (D. Eckardt), harold.cremer@ibdml.univmed.fr (H. Cremer), AndreasBo@miltenyibiotec.de (A. Bosio).
[1] Present address: IBDML-CNRS-UMR 7288, Case 907- Campus Universitaire et Technologique de Luminy, Route Léon Lachamp, 13288 Marseille Cedex 09, France.
[2] IBDML-CNRS-UMR 7288, Case 907- Campus Universitaire et Technologique de Luminy, Route Léon Lachamp, 13288 Marseille Cedex 09, France.
[3] Present address: HydroSciences Montpellier Unité Mixte de Recherche 5569 16 Rue Charles Bonaparte, 34080 Montpellier, France.
[4] IBDML-CNRS-UMR 7288, Case 907- Campus Universitaire et Technologique de Luminy, Route Léon Lachamp, 13288 Marseille Cedex 09, France. Fax: +33 4 91 26 93 16.

1873-5061/$ - see front matter
http://dx.doi.org/10.1016/j.scr.2012.10.005

enrichment of neuronal precursors based on PSA-NCAM expression represents a general and straightforward approach to narrow cellular heterogeneity during neuronal differentiation of pluripotent cells.

Introduction

Pluripotent stem cells hold the potential to generate all cell types in culture, but the development of methods which control differentiation to induce generation of one cell type over another has proved challenging. The differentiation of mouse and human pluripotent stem cells into specific neural subpopulations has been achieved using determined extracellular environments, specific signaling factors, small molecules, co-culture systems, or transgenic modifications (Chung et al., 2002; Friling et al., 2009; Kawasaki et al., 2000; Lee et al., 2000; Martinat et al., 2006; Okabe et al., 1996; Tropepe et al., 2001; Wichterle, et al., 2002; Ying, et al., 2003). However, despite the general progress in differentiation strategies, several aspects are still insufficiently understood, especially when aiming at pluripotent cell-derived neurons for regenerative approaches. For example, lack of synchronicity and purity of the target cell population represent two major limitations. Target cells should fit into a specific developmental window since implantation of pre-differentiated and proliferative cells can give rise to slow-growing tumors (Roy et al., 2006), while cells too advanced in their differentiation may be unable of functional integration (MacLaren et al., 2006). Moreover, the presence of undifferentiated pluripotent cells must be avoided to prevent teratoma formation upon *in vivo* injection (Bjorklund et al., 2002; Thomson et al., 1998).

Cell sorting strategies have been suggested as one way to address these issues (Sharp and Keirstead, 2009). Accordingly, specific cell surface markers and the respective antibodies have been reported for undifferentiated pluripotent cells as well as for differentiated neural cells, both in humans and rodents (Golebiewska, et al., 2009; Pruszak, et al., 2009; Pruszak, et al., 2007). In addition, several flow cytometer and magnetic bead based protocols using a combinatorial surface antigen code have been applied to enrich ES-derived neural precursors (Chung et al., 2011; Pruszak, et al., 2009, 2007; Yuan et al., 2011). Depending on the target cell number and the need for a closed, sterile procedure, magnetic sorting rather than flow sorting has been reported to allow for a faster separation and gentler handling of cells, and operations under sterile conditions (Bosio et al., 2009; Pruszak, et al., 2007).

The polysialylated acid (PSA) was described as a major macromolecular component of the vertebrate brain (Finne, 1982) being attached exclusively to the cell surface glycoprotein neural cell adhesion molecule (NCAM) (Cremer et al., 1994; Finne, et al., 1983). The neuroanatomical distribution of PSA-NCAM differs between the developing and adult nervous system. PSA-NCAM expression peaks in the late embryonic and post-natal developing nervous system (Finne, 1982) and is considered a marker for immature neural precursors (Nguyen, et al., 2003). In the adult brain, NCAM displays low levels of polysialylation (Angata and Fukuda, 2003) with the exception of areas that show ongoing neurogenesis, such as the subventricular zone–rostral–migratory stream–olfactory bulb system and the hippocampal dentate gyrus (Durbec and Cremer, 2001; Rousselot, et al., 1995). In general, PSA-NCAM is considered a promoter of neural plasticity, allowing migration and facilitating axonal pathfinding, synaptogenesis (El Maarouf and Rutishauser, 2003; Kiss and Rougon, 1997) and synaptic plasticity (Cremer et al., 1998; Muller et al., 1996). The level of PSA-NCAM has been shown to increase in chronic stress conditions (Pham, et al., 2003) and lesion models as ischemia, epilepsy, brain trauma, and transected/crushed peripheral nerves (Bonfanti et al., 1996; Franz, et al., 2005; Rutishauser and Landmesser, 1996). Based on these properties it has been proposed that PSA-NCAM expressing cells hold potential for promoting brain repair (El Maarouf, et al., 2006; Franz, et al., 2005; Nguyen, et al., 2003) and neuroprotection (Duveau, et al., 2007).

In this study we analyzed PSA-NCAM expression during neuronal differentiation of pluripotent mESC and developed a method for isolation of the PSA-NCAM positive precursor population by immunomagnetic sorting. Based thereon we investigated if PSA-NCAM-mediated enrichment is suited to decrease heterogeneity of *in vitro* generated neuronal precursors. We then characterized the differentiation potential of the PSA-NCAM-enriched neural precursors *in vitro* and observed an increase in the number of neuronal cells at the end of the differentiation process. In order to analyze if PSA-NCAM enriched cells could behave as *in vivo* neuroblast, we stereotactically injected the sorted population into the forebrain of adult mice. Here, PSA-NCAM$^+$ mESC derived neuronal precursors showed efficient migration and predominant differentiation into NeuN positive neurons. In summary we showed that a straightforward *in vitro* enrichment of ES cell derived neuronal precursor cells can be used to promote neuronal differentiation and to increase grafting efficiency *in vivo*.

Material and methods

Animals

Two month old C57BL/6 mice were purchased from Charles River and used as host animals. Animals were housed under standard conditions with access to water and food *ad libitum* on a normal 12 h light/dark cycle. Experiments were performed in accordance with the principles for laboratory animals published by the French Ethical Committee.

Mouse ES cell culture and *in vitro* differentiation

Actin-eGFP C57BL/6 mESCs were propagated on Mitomycin-C (Sigma-Aldrich, Steinheim, Germany, http://www.sigmaaldrich.com)-treated mouse fibroblasts in DMEM (Miltenyi Biotec, Bergisch Gladbach, Germany, http://www.miltenyibiotec.com) supplemented with 1 mM nonessential amino acids (PAA, Cölbe, Germany, http://www.paa.com/), 1× Na Pyruvate (PAA), 2 mM L-Glutamine (PAA) 0.1 mM b-Mercaptoethanol, 1% Penicillin Streptomycin (PAA), 10% FCS

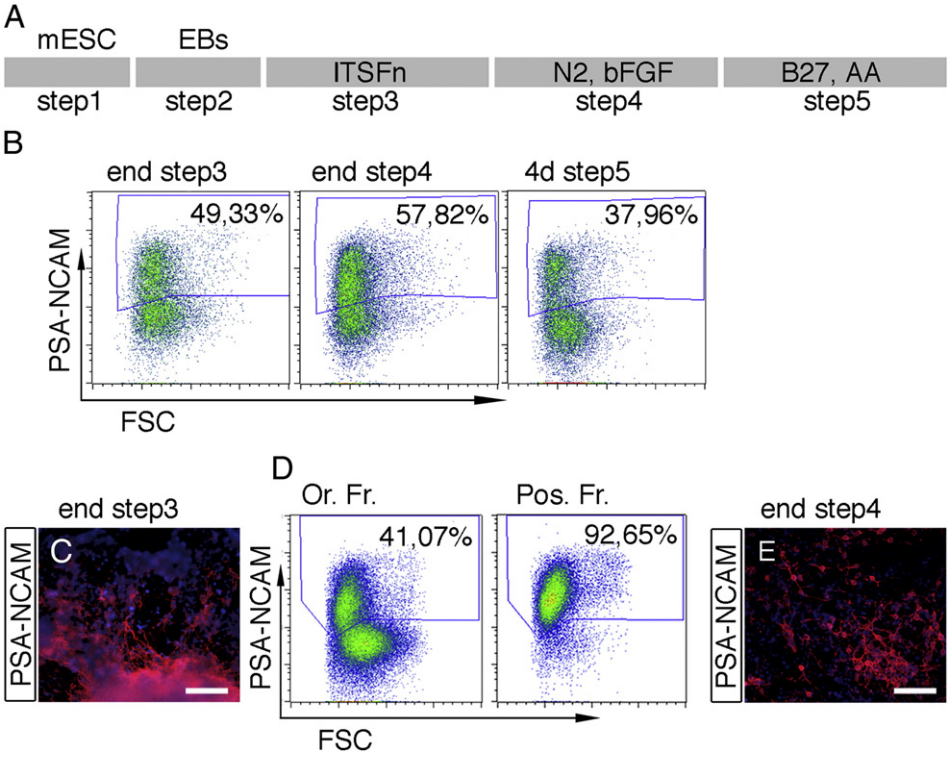

Figure 1 *In vitro* differentiation and immunomagnetic enrichment of mESC derived PSA-NCAM$^+$ neural precursors. (A) Schematic representation of neural differentiation. (B) Flow cytometric analysis of PSA-NCAM expression during neural differentiation. (C, E) Immunofluorescence microscopy of *in vitro* derived PSA-NCAM$^+$ precursors (red) before (C) and after magnetic separation (E), nuclei stained with DAPI (blue). (D) Intensity distribution of PSA-NCAM$^+$ cells before (Ori. Fr.) and after (Pos. Fr.) magnetic cell sorting. Scale bar = 50 μm. Abbreviations: mESC, mouse embryonic stem cells; EBs, embryoid bodies; ITSFn, insulin transferrin selenium fibronectin; bFGF, basic fibroblast growth factor; AA, ascorbic acid; PSA-NCAM, polysialylated neural cell adhesion molecule; FCS, forward scatter; Ori. Fr., original fraction; Pos. Fr., positive fraction.

(PAA) and 0.01% LIF (Miltenyi Biotec) (step 1). Cells were split every two days and plated at a concentration of 25,000/cm^2. Before embryoid bodies (EBs) differentiation (step 2), cells were harvested with 0.05% Trypsin (Sigma), subjected to feeder depletion with Feeder Removal MicroBeads Kit (Miltenyi Biotec) and then plated on non-adherent bacterial dishes for four days in LIF free EB medium containing 5% of knockout serum replacement (Invitrogen, Frederick, MD, http://www.invitrogen.com) and 5% FCS (PAA). EBs were then plated onto adhesive tissue culture surface. After 24 h in culture, selection of neural progenitor cells was initiated in serum-free 1× ITS liquid media supplements (Sigma-Aldrich) plus 5 mg/ml Fn (Biopure, Bubendorf, Switzerland, http://www.biopur.com/index.php) supplemented with DMEM medium (ITSFn, step 3). After 6 days (6 d) of selection, cells were harvested with AccuMax (PAA), plated on polyornithine (Sigma-Aldrich) and laminin (Sigma-Aldrich) coated 24 well plates and cultivated for 5 d (step 4) in MACS Neuro Medium (Miltenyi) supplemented with 1× N_2 supplement (PAA), 1 mM nonessential amino acids, 2 mM L-Glutamine, 1% Penicillin Streptomycin, 1 mg/ml laminin, and 10 ng/ml bFGF (Miltenyi). For neuronal differentiation (step 5) bFGF was removed to induce differentiation, N_2 supplement was substituted with 1× B27 (PAA) supplement and 200 mM ascorbic acid was added. Cells were cultivated in neuronal differentiation medium for 7 d.

Flow cytometric analysis

Single cell suspensions obtained at different steps of the neuronal differentiation protocol were stained with anti-PSA-NCAM–APC antibody (Miltenyi Biotec) for flow cytometric analysis. 1×10^6 cells were incubated 10 min at 4 °C with the conjugated antibody.

Cell debris and dead cells (identified by propidium-iodide) were excluded from the analysis. Data was acquired on a MACSQuant Analyzer (Miltenyi Biotec). PSA-NCAM positivity was determined according to negative controls where no primary antibody was used and by comparing to undifferentiated Actin-eGFP C57BL/6 mESCs which do not express PSA-NCAM.

Magnetic labeling and cell isolation

Cell suspensions containing approximately 3×10^6 cells were first labeled with anti-PSA-NCAM antibody conjugated to APC fluorochrome (Miltenyi Biotec). Then magnetic MicroBeads coupled to anti-APC antibody were applied. Cells were re-suspended in mESC medium and the cell suspension was loaded onto an MS-column (Miltenyi Biotec), which was placed in the magnetic field of a MACS Separator. The column was rinsed three times with 0.5 ml of medium. Magnetically isolated PSA-NCAM positive cells were retained in the column and eluted as the positively selected cell fraction after

removing the column from the magnet. Immunomagnetic removal of dead cells prior to enrichment with anti-PSA-NCAM was performed using the Dead Cell Removal Kit (Miltenyi Biotec).

Isolated *in vitro* derived PSA-NCAM positive cells were seeded on polyornithine and laminin coated 24-well plates and further differentiated into neuronal lineage as describe above for *in vitro* analysis or were collected in medium at a concentration of 50,000/ml and used for transplantation.

Immunocytochemistry and statistical analysis

For immunofluorescence staining, cells were fixed in 4% paraformaldehyde (Sigma-Aldrich-Aldrich) for 10 min, rinsed with PBS, and then incubated with blocking buffer (PBS, 4% bovine serum albumin) with or without 0.1% Triton (for intracellular and surface markers respectively) for 30 min. Cells were then incubated 1 h at room temperature with the primary antibodies diluted in blocking buffer solution. The following primary antibodies were used: mouse anti-nestin (1:200, Santa Cruz Biotechnology, Santa Cruz, CA, U.S.A., http://www.scbt.com/), mouse anti-PSA-NCAM (1:500, Miltenyi Biotec), mouse anti-Oct4 (1:50, Santa Cruz Biotechnology), mouse anti-Ki67 (1:100, BD Pharmingen, Heidelberg, Germany, http://www.bdbiosciences.com/eu/index.jsp), mouse anti-TUJ1 (1:500, Covance, Princeton, New Jersey, http://www.covance.com/), mouse anti-MAP2 (1:200, Millipore, Billerica, MA, U.S.A., http://www.millipore.com/), mouse anti-GAD67 (1:1000, Millipore), mouse anti-NeuN (1:100, Millipore), mouse anti-GFAP (1:500, Millipore), rabbit anti-Olig2 (1:500, Millipore), mouse anti-synaptophysin (1:200, Sigma-Aldrich-Aldrich), and rabbit anti-VGlut-1 (1:500, Synaptic Systems, Göttingen, Germany, http://www.sysy.com/). After additional rinsing with PBS, samples were incubated with fluorescent-labeled secondary antibody Alexa 594 anti-mouse-IgG and IgM (1:400, Invitrogen) in blocking solution

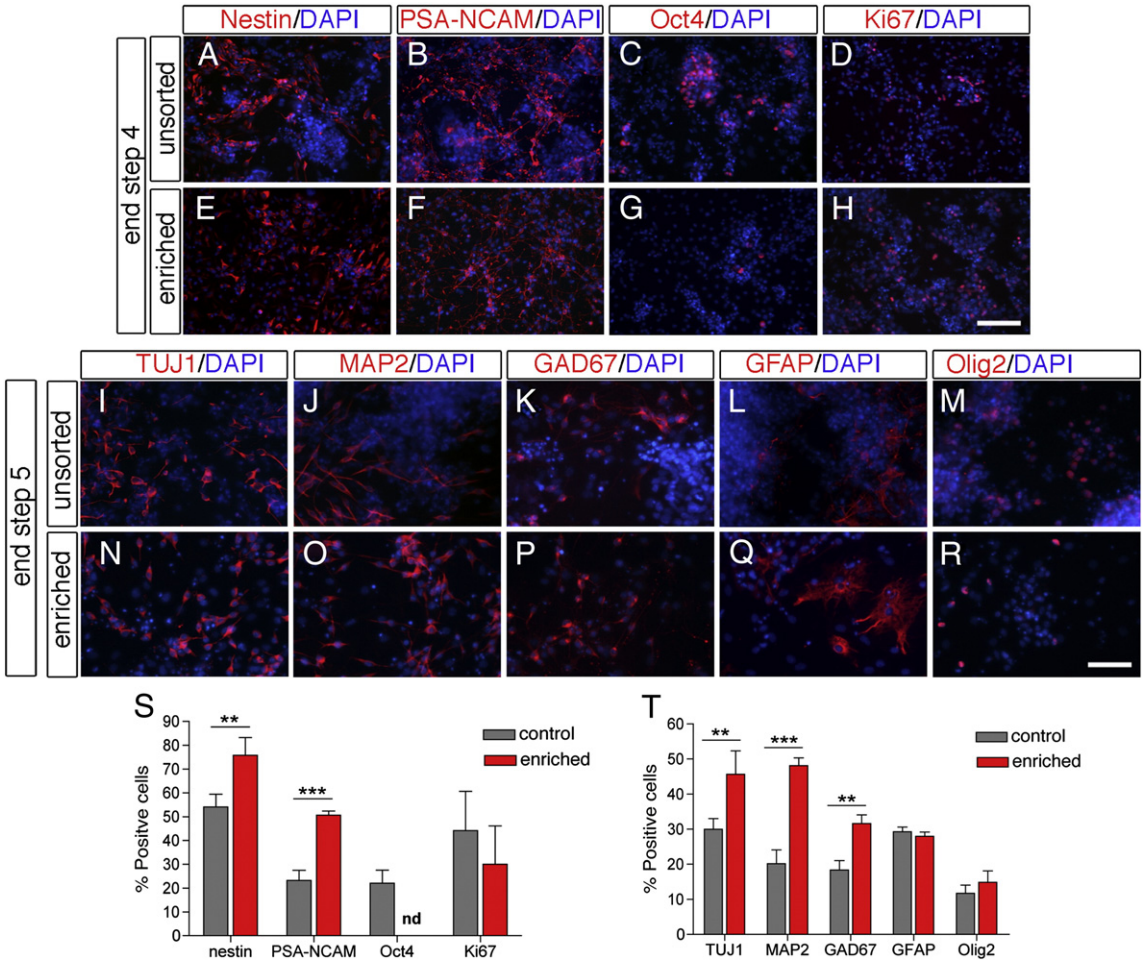

Figure 2 PSA-NCAM enrichment improves *in vitro* neuronal differentiation. (A–H) Immunocytochemistry at differentiation step 4 (day 16) of unsorted control population (upper panels) *versus* PSA-NCAM enriched population (lower panels). Cells stained for (A, E) nestin (red), (B, F) PSA-NCAM (red), (C, G) Oct4 (red), and (D, H) Ki67 (red). Nuclei stained with DAPI (blue). (I–R) Immunocytochemistry at step 5 (differentiation day 23) of unsorted control population (upper panels) *versus* PSA-NCAM enriched population (lower panels). Cells stained for (I, N) TUJ1 (red), (J, O) MAP2 (red), (K, P) GAD67 (red), (L, Q) GFAP (red), and (M, R) Olig2 (red). Nuclei stained with DAPI (blue). (S, T) Quantification of the data presented in A–R; mean ± S.E.M., $n=4$ (independent experiments): ***$P<0.0001$; **$P<0.01$. Scale bar = 100 μm (upper), 50 μm (lower). Abbreviations: PSA-NCAM, polysialylated neural cell adhesion molecule; Oct4, octamer-binding transcription factor 4; MAP2, microtubule-associated protein 2; GAD67 glutamic acid decarboxylase 67; GFAP glial fibrillary acidic protein; Olig2, oligodendrocyte transcription factor 2; nd, not detectable.

buffer for 45 min at room temperature. After rinsing with PBS, DAPI was used for counterstaining. Immunocytochemical control consisted in omission of the primary antibodies.

Images were acquired using Nikon Eclipse TS 100 fluorescence microscope. Four independent control *vs* enriched experiments were considered and for each staining up to 6–8 images were acquired randomly and 750 nuclei were counted. For statistical analysis we used the Prism software and performed two-tailed unpaired t-test, error bars represent the SD.

Transplantation and immunohistofluorescence

Neural progenitors-mESC-derived were harvested with AccuMax after 6 d selection in serum free ITSFn supplemented medium. Cells were then processed for PSA-NCAM enrichment (see above). The positive fraction as well as the unsorted population were resuspended in medium at a concentration of 50,000 cells/μl. 1 μl was injected into forebrain of C57BL/6 (n=15 for each condition) at the level of the RMS (from the bregma: 2.5 mm anterior, 0.9 mm lateral and 2.4 mm deep) using a Kopf apparatus and a 2 μl Hamilton syringe. After 10 or 40 days post-grafting (dpg), the animals were perfused intracardially with 4% paraformaldehyde solution in phosphate buffer (PB). Brains were dissected out, post-fixed for 24 h and serial sagittal or coronal sections (50 μm) were obtained with a vibratome (Microm, Walldorf, Germany, http://www.microm-online.com/). Free-floating sections were then incubated for 1 h at room temperature in 3% BSA/PB and afterwards incubated overnight at 4 °C in fresh blocking solution containing a mixture of chicken or mouse antiGFP (1:500, Aves labs, Tigard, Oregon, USA, http://www.aveslab.com/, and Millipore respectively) antibody and chicken anti-nestin (1:200, Aves labs), or mouse anti-PSA-NCAM (1:250, Miltenyi Biotec), mouse anti-TUJ1 (1:500, Covance), mouse anti-NeuN (1:100, Millipore), mouse anti-GFAP (1:500, Millipore), rabbit anti-Olig2 (1:500, Millipore), and anti-GLAST (ACSA-1) (1:500, Miltenyi Biotec).

The sections were then washed in 0.1% Triton-PBS (PBT) and incubated in blocking solution with the corresponding secondary antibody for 1 h at room temperature (anti-chicken Alexa 488, anti-mouse-IgG Alexa 488, anti-chicken Alexa 647, anti-mouse-IgG or IgM Alexa 594, and anti-rabbit Alexa 594, 1:400, Invitrogen). Hoechst was used for counterstaining. Subsequently, the sections were washed, transferred to slides and air-dried. Immunofluorescence controls consisted in omission of the primary antibodies. Fluorescence was detected using a confocal laser-scanning microscope Leica TCS SP II (Leica, Wetzlar, Germany, http://www.leica-microsystems.com/) equipped with an Ar and HeNe lasers. Single z-stack sections were captured with sequential image acquisition in order to avoid spectral cross-talk. For quantification, one section each of 3 animals was randomly chosen for each marker considered. Single z-stack sections were captured over the complete graft area, and 500 GFP^+ cells were counted. For statistical analysis we used the Prism software and performed two-tailed unpaired t-test, error bars represent the SD.

Microarray analysis

1×10^6 cells were harvested, rapidly frozen in liquid nitrogen and stored at −70 °C. Three biological replicates were processed for each condition.

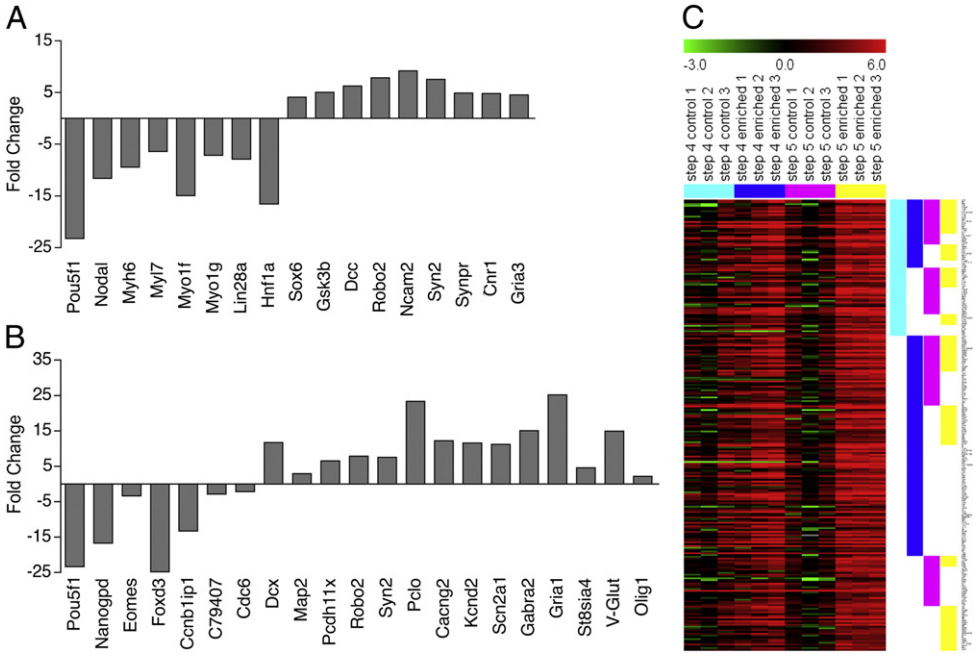

Figure 3 Gene expression profile of neuronal differentiated PSA-NCAM enriched precursors. (A, B) Gene expression fold change of PSA-NCAM enriched population relative to control population at step 4 (A, differentiation day 16) and step 5 (B, differentiation day 23). (C) Compressed heatmap of upregulated genes in PSA-NCAM enriched population at step 5 (annotations legend: light blue — synapse; dark blue — nervous system development; magenta — transmission of nerve impulse; yellow — neuron projection). Biological triplicates of control and PSA-NCAM enriched population at step 4 and step 5 are shown.

RNA was isolated using standard RNA extraction protocols (Trizol). RNA quality and integrity were determined using the Agilent RNA 6000 Nano Kit on the Agilent 2100 Bioanalyzer (Agilent Technologies, Böblingen, Deutschland, http://www.home.agilent.com/agilent/home.jspx?cc=DE&lc=ger). RNA was quantified by measuring $A_{260\ nm}$ on the ND-1000 Spectrophotometer (NanoDrop Technologies, Wilmington, DE, USA, http://www.nanodrop.com/). Sample labeling and hybridization was performed as detailed in the "Two-Color Microarray-Based Gene Expression Analysis protocol" (Agilent).

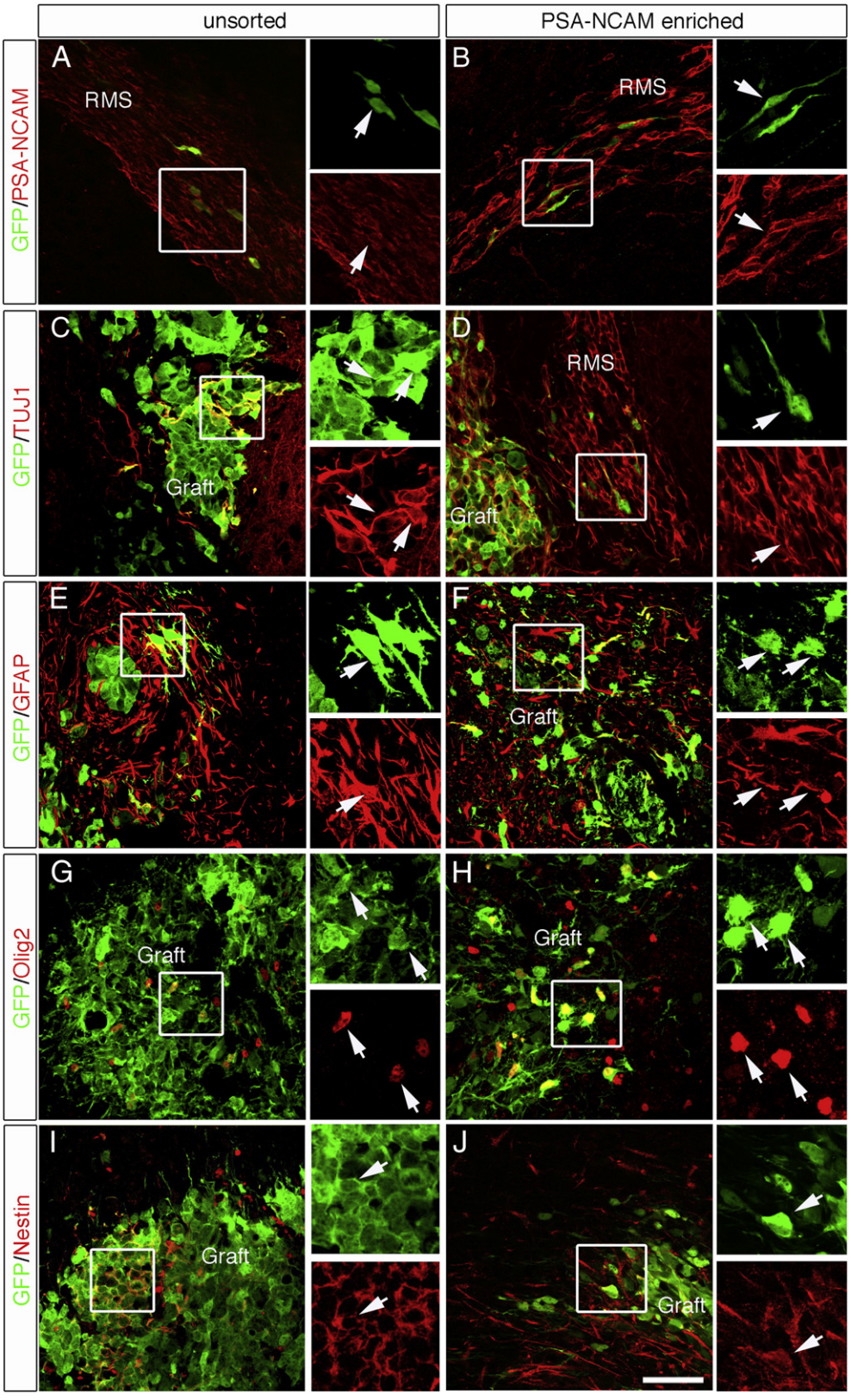

Fluorescence signals of the hybridized Agilent Microarrays were detected using Agilent's Microarray Scanner System G2505B with a resolution of 5 μm. The Agilent Feature Extraction Software (FES) version 10.7.3.1 was used to read out and process the microarray image files. For determination of differential gene expression, FES derived output data files were further processed using the Rosetta Resolverâ gene expression data analysis system (Rosetta Biosoftware).

All microarray data have been deposited in NCBI's Gene Expression Omnibus7 and are accessible through GEO Series accession number GSE35125 (http://www.ncbi.nlm.nih.gov/geo/query/acc.cgi?token=rzezjaoycqwcmtc&acc=GSE35125).

Differentially expressed genes were identified by a combination of effect size and statistical significance based on the Cy5 channel data. Only genes with an at least six-fold upregulation in "step 5 enriched" samples compared to "step 5 control" samples and an unadjusted P-value (two-tailed t-test, equal variance) of less than or equal to 0.05 were subjected to annotation enrichment analysis using the TreeRanker tool (Miltenyi Biotec). Term enrichment relative to the expected background distribution was scored using Fisher's exact test. Annotations were derived from publicly available and literature-derived data sources, *e.g.* Gene Ontology (GO, www.geneontology.org), signaling pathway membership, sequence motifs, literature keywords, and cell-specific marker genes.

Results

Immunomagnetic enrichment of mESC-derived PSA-NCAM$^+$ neural precursors

In order to analyze PSA-NCAM expression during *in vitro* neuronal differentiation of mESCs, we used a well-established embryoid body (EB)-based five-step differentiation protocol (Lee, et al., 2000), which recapitulates early embryonic development (Fig. 1A). To facilitate tracing of cells in transplantation studies, mESC derived from actin-eGFP C57BL/6 transgenic mice (Hadjantonakis, et al., 1998) (Fig. S1A) was used. Flow cytometry analysis revealed that at the end of step 3 of the differentiation protocol about 95% of the cells were e-GFP positive (Fig. S1B). We evaluated PSA-NCAM expression at three time points using flow cytometry (gating strategy is represented in Figs. S2A–D). PSA-NCAM was already detectable at the end of the differentiation step 3, after ITSFn selection for neural precursors (Fig. 1B). Immunocystochemistry analysis showed a predominant location of PSA-NCAM$^+$ cells within the cells exiting from the plated EB aggregates (Fig. 1C). PSA-NCAM frequency increased at the end of step 4. In the course of the final differentiation step, when withdrawal of mitogen from medium cultivation triggers a post-mitotic fate in the developing neuronal progenitors (4 days in step 5), the frequency of PSA-NCAM$^+$ cells decreased (Fig. 1B).

To test whether an enrichment of mESCs derived PSA-NCAM$^+$ cells would increase neuronal differentiation, we developed a protocol for isolation of the PSA-NCAM positive fraction by magnetic cell sorting. The isolation protocol was applied at step 3, the first time point when PSA-NCAM expression was observed. Cells were harvested and labeled with anti-PSA-NCAM–APC antibody followed by anti-APC MicroBeads. Flow cytometric analysis showed an initial frequency of 41.07 ± 7.95% PSA-NCAM positive cells (Or. Fr., Fig. 1D). Magnetic cell sorting enriched PSA-NCAM positive cells to 92.65 ± 1.86% (Pos. Fr., Fig. 1D) and did not impede subsequent cultivation of sorted cells (Fig. 1E). However, we observed that binding of the anti-PSA-NCAM antibody and, therefore, sorting efficiency was impaired by high levels of cellular debris (Fig. S3A). This was specifically prominent when starting frequency of PSA-NCAM$^+$ cells was low (18.56 ± 5.73%). For this reason we included an immunomagnetic removal of dead cells prior to enrichment with anti-PSA-NCAM. As shown in Fig. S3B, this eventually allowed us to achieve a high purity (93.52 ± 0.96%) of PSA-NCAM$^+$ cells.

PSA-NCAM is not exclusively expressed in CNS. For instance, β^{high}- and β^{low}-pancreatic cells have been characterized based on differential PSA-NCAM expression (Karaca et al., 2009). In order to investigate the potential contamination of pancreatic endocrine cells among the PSA-NCAM$^+$ cells, we analyzed the gene expression profile of the PSA-NCAM positive fraction using whole genome micro array. We then queried for pancreas-associated genes based on Gene Ontology annotation and found that 34 pancreas-associated genes, were upregulated in the PSA-NCAM positive fraction as compared to undifferentiated mESC. However it is well-known that all this 34 genes are also expressed in neural development as FoxA2, NeuroD1, Pax6, Sox9, Isl1 and Nkx6.1. Pancreatic endocrine cells share a high number of expressed genes with neurons and pancreatic development is driven by many transcription factors which are described in neural development. Genes expressed in neural precursors were upregulated in the PSA-NCAM positive fraction as Dcx, Sox1, Robo2, TUBB3, and Ascl1 (Fig. S4A). We then searched for the expression of genes known to be involved in pancreatic islet development and maintenance as Sox17, Pdx1, Hlxb9, Pax4, Ptf1a, Hnf4, Hnf6, and Gata4. Except for Hnf6 that appears 3 fold downregulated, not one of the other genes was found. Finally we analyzed by immunofluorescence the presence of Sox17, a well known marker for definitive endoderm. While we were able to detect few positive cells at the end of the differentiation step 3 (before PSA-NCAM enrichment) (Fig. S4B),

Figure 4 *In vivo* characterization of mESC derived neural precursors and PSA-NCAM enriched progenitors after 10 days post graft. (A, B) Grafted GFP$^+$ cells (green), immunopositive for PSA-NCAM (red) both in the unsorted (A) and PSA-NCAM enriched population (B). GFP$^+$ cells are integrated in the RMS and show typical surface PSA-NCAM staining (see insets, arrows). (C–D) Double immunopositive cells for GFP (green) and TUJ1 (red) detected in the graft core and in the RMS both in unsorted and PSA-NCAM enriched population (left and right images, insets, arrows, respectively). (E, G) Unsorted population, immunohistochemistry for GFP (green) and co-expression (red) with GFAP (E) and Olig2 (G). (F, H) PSA-NCAM enriched population (green) expressing GFAP (F, red) and Olig2 (H, red). (I, J) Grafted cells from unsorted and enriched population (I and J respectively, green) double positive with nestin (blue). Arrows in insets: double positive cells. Scale bar = 50 μm. Abbreviations: GFP, green fluorescent protein; PSA-NCAM, polysialylated neural cell adhesion molecule; GFAP glial fibrillary acidic protein; Olig2, oligodendrocyte transcription factor 2; RMS, rostral migratory stream. 3–4 animals were analyzed for each marker.

after 24 h plating, only few Sox17$^+$ positive cells were found in the PSA-NCAM negative, and no immunopositive cells were detected in the PSA-NCAM positive fraction (Fig. S4C).

In vitro differentiation of mESC derived PSA-NCAM$^+$ precursors

In order to evaluate the lineage propensity of PSA-NCAM$^+$ cell fraction, sorted cells were further differentiated following the above mentioned protocol. After neural progenitor expansion (step 4), the PSA-NCAM enriched population gave rise to a significantly higher number of nestin and PSA-NCAM expressing cells as compared to the unsorted control population with 75.75 ± 7.48% *vs.* 54.08 ± 5.34% nestin$^+$ cells and 50.69 ± 1.74% *vs.* 23.24 ± 4.23% PSA-NCAM$^+$ cells, respectively (Figs. 2A, B, E, F, S). This indicated that the ES cell derived PSA-NCAM sorted cells were indeed enriched for neural precursors. To further assess the differences in the differentiation of cells after PSA-NCAM enrichment, we stained for Ki-67 and Oct4 expression. We observed a slight though statistically not significant reduced number of proliferating Ki-67 positive cells in the PSA-NCAM enriched cell population (Fig. 2S; 44.11 ± 16.53% *vs.* 29.14 ± 16.17% Ki-67$^+$ cells for unsorted *vs.* enriched cells). The number of residual Oct4 positive cells was strongly reduced in the PSA-NCAM enriched population (<10 cells per 24 well plate; Figs. 2C, G, S), indicating highly efficient removal of potentially teratoma-forming pluripotent stem cells. After neuronal differentiation (step 5), the PSA-NCAM enriched population gave rise to a significantly increased number of cells with neuronal characteristics as indicated by the expression of the early post-mitotic marker TUJ1or the later expressed neuronal proteins, MAP2 and GAD67 (Figs. 2I–K, N–P, T; 29.98 ± 3.02% *vs.* 45.69 ± 6.64% TUJ1$^+$ cells, 21.87 ± 3.47% *vs.* 48.13 ± 2.21% MAP2$^+$ cells and 18.37 ± 2.67% *vs.* 31.65 ± 2.45% GAD67$^+$ cells for unsorted *vs.* enriched cells). Some cells also expressed NeuN (Fig. S5A), while only few cells were TH$^+$ (data not show). Notably, in both the unsorted and PSA-NCAM enriched population, we were able to detect expression of synaptophysin, a marker for vesicular synapses (Fig. S5B).

In contrast, the number of GFAP or Olig2 positive glial cells was similar in the control and the PSA-NCAM enriched population (Figs. 2L, M, Q, R, T; 29.26 ± 1.38% *vs.* 27.97 ± 1.22% GFAP$^+$ cells and 11.71 ± 2.39% *vs.* 14.86 ± 3.25% Olig2$^+$).

To further delineate the differences between the PSA-NCAM enriched and control cells, we analyzed the gene expression of both populations at steps 4 and 5 of differentiation using whole genome arrays. Differentially expressed genes were first grouped according to their functional annotation. Already at differentiation step 4, the PSA-NCAM enriched population showed a higher presentation of genes involved in neuron development (*e.g.* Sox6 and Gsk3b), and more specific, genes included in synaptic transmission (*e.g.* Syn2 and Synpr), neuron differentiation, axogenesis (*e.g.* Dcc, Robo2, and Ncam2), and regulation of neurotransmitter levels (*e.g.* Cnr1 and Gria3) (Fig. 3A). A smaller proportion of the differentially expressed genes was reduced in the enriched population and most of them mapped to biological terms related to pluripotency and development (*e.g.* Pou5f1, Nodal, and Lin28a) of non-neuronal lineages (*e.g.* Myh6, Myl7, Myo1f, Myo1g, Lin28a, and Hnf1a) (Fig. 3A). The enrichment of genes involved in neuronal development, detected in the PSA-NCAM$^+$ fraction at step 4 became more prominent at the end of neuronal differentiation. Here, the gene expression profile showed up-regulation of genes exclusively involved in neural, and particularly neuronal, activity (Fig. 3C). For example, we found enrichment of biological terms such as synapse (representative genes: Pcdh11, Syn2, and Pclo), nervous system development (representative genes: Dcx, Map2, and St8sia4), transmission of nerve impulse (representative genes: Gabra2 and Gria1), neuron projection, ion channel complex, ion transmembrane transporter, voltage gated cation channel activity (representative genes: Cacng2, Kcnd2, and Scn2a1), regulation of action potential, glutamate signaling pathway (represented here by the gene V-Glut), and GABA receptor activity (represented here by the gene Gabra2) (Fig. 3B). Genes involved in pluripotency, like Pou5f1 (Oct4) and Nodal, were still present in the PSA-NCAM enriched population at low levels (Fig. 3B). Moreover, we found an under-representation of biological terms related to development (representative genes: Eomes and Foxd3) and proliferation (representative genes: Ccnb1ip1, C79407, and Cdc6).

PSA-NCAM enriched neural precursors survive *in vivo* and differentiate into neurons.

We next compared the *in vivo* differentiation potential of unsorted and enriched PSA-NCAM$^+$ cells. Actin-GFP C57BL/6 mESCs were differentiated and purified using PSA-NCAM immunoreactivity as described above (Immunomagnetic enrichment of mESC-derived PSA-NCAM$^+$ neural precursors section). The unsorted and the PSA-NCAM positive populations were stereotactically injected into the forebrain of adult mice. After 10 days post graft (dpg), grafted cells were distributed between layer 1 of the somatomotor cortex and the more ventral curve of the RMS (dorsal–ventral axis), and between the orbital areas rostrally and the fiber tract, caudatoputamen and lateral ventricle caudally. The phenotype and differentiation of grafted cells were analyzed at 10 or 40 dpg. Double staining for transgenic-GFP, and several markers for neuronal (PSA-NCAM, TUJ1, NeuN, and MAP2), glial (GFAP, GLAST, and Olig2), or neural stem cells (nestin) was performed.

Ten days post-grafting, PSA-NCAM enriched cells showed a high level of PSA-NCAM and TUJ1-immunoreactivity within the graft area as shown by quantification of the immunofluorescence (Fig. S6A; GFP$^+$/PSA-NCAM$^+$ 29.51 ± 8.96% and GFP$^+$/TUJ1$^+$ 40.2 ± 2.75%). PSA-NCAM and TUJ1 positive cells were found mainly in the central area of the graft, where they tended to reside in clusters. In addition, some GFP$^+$/PSA-NCAM$^+$ or GFP$^+$/TUJ1$^+$ cells were also found in the rostral migratory stream (RMS), a structure that contains high numbers of PSA-NCAM/TUJ1 positive migratory neuroblasts in the adult (Bonfanti and Theodosis, 1994) (Figs. 4B, D). In contrast, only few cells in the unsorted population were GFP$^+$/PSA-NCAM$^+$ or GFP$^+$/TUJ1$^+$. Notably, only few GFP$^+$/TUJ1$^+$ cells were located in the graft area (Fig. S6A 7.49 ± 3.88%), while most resided in the RMS (Fig. 4C). GFP$^+$/PSA-NCAM$^+$ cells were located in the RMS and not in the graft

area (Fig. 4A). Next, we analyzed the expression of astrocyte markers GFAP and GLAST and the oligodendrocyte marker Olig2 (Figs. 4E–H). We found all three markers on grafted cells derived from the PSA-NCAM enriched as well as the control population (Fig. S6A 11.95 ± 5.59% *vs.* 9.22 ± 6.04% GFAP$^+$ cells and 6.71 ± 4.81% *vs.* 11.46 ± 3.24% Olig2$^+$ cells for unsorted *vs.* enriched cells). Notably, Olig2 positive cells were located within as well as outside the graft area, indicating migration of these cells into the host tissue, which contrasts the behavior of GFP$^+$/GFAP$^+$ that were always retained in the graft area. We also observed an intense GFAP and GLAST staining around the graft mass, which did not co-localize with GFP probably related to a host gliosis reaction. The neural stem cell marker nestin was detected in both populations (Figs. 4I, J) even if in the PSA-NCAM enriched population the GFP$^+$/nestin$^+$ cells were significantly lower than in the unsorted population (Fig. S6A 11.46 ± 4.2% *vs.* 1.82 ± 2.28% nestin$^+$ cells for unsorted *vs.* enriched cells). Interesting, considering the glial markers (GFAP and Olig2) and neuronal marker (TUJ1) we found that after 10 dpg only a small portion of the cells in the unsorted population were neural and mainly of glial lineage, while in the PSA-NCAM enriched population more than the 60% were neural with predominance of TUJ1$^+$ cells (Fig. S6B). Importantly, we were not able to detect GFP positive cells that expressed the mature neuronal marker NeuN in both, the PSA-NCAM enriched and the unsorted population.

However, forty days post grafting the PSA-NCAM enriched as well as the not enriched control population showed expression of NeuN (Figs. 5A, K). At this time point, grafted cells were distributed throughout all neuronal layers of the frontal cortex. Notably, while in the unsorted population a relatively small number of the cells were GFP$^+$/NeuN$^+$ (14.1 ± 7.6%), a much higher number of cells in the PSA-NCAM enriched population showed NeuN-immunoreactivity (69.1 ± 6.5%) (Fig. 5b). In line with this observation, unsorted ES derived GFP$^+$ cells were still PSA-NCAM or TUJ1-immunoreactive (Figs. 5B–G), while no GFP/PSA-NCAM double positive cells and only few GFP/TUJ1 double positive cells were detected in the PSA-NCAM enriched population (Figs. 5L–R). The percentage of cells immunoreactive for the glial markers GLAST, GFAP, or Olig2 was comparable in both grafted populations (Figs. 5H–J, S–a).

Importantly, in case of control cell grafting, 7 out of 15 animals showed a severe damage of the host neural tissue at 10 dpg. In particular, in these animals the tissue surrounding the injection site, covering half of the frontal hemisphere, came off in a single block during dissection. In the remaining animals the volume of the graft was comparable to animals where PSA-NCAM enriched population was grafted (0.107 ± 0.045 mm^3 *vs.*0.079 ± 0.047 mm^3, mean ± SD n = 3 mice; Figs. S7A–D). Between 10 and 40 dpg, 3 animals died and at 40 dpg, we detected an extensive cellular overgrowth in 4 of the animals where control cells were transplanted. None of the 15 animals where PSA-NCAM enriched cells were transplanted showed damage of the neural tissue at 10 dpg and only one animal died between 10 and 40 dpg. Rosettes like structures indicating tumor formation were observed in only 1 animal at 40 dpg.

Cells immunopositive for the cell cycle marker Ki67$^+$ were detected in both unsorted and PSA-NCAM enriched populations at 10 dpg (Figs. S7E, F).

Migration of PSA-NCAM *in vitro* derived neural precursors.

We demonstrated in a previous study that after homotypic transplantation of SVZ tissue from actin-EGFP transgenic adult donor mice, graft-derived cells underwent migration and differentiation indistinguishable from endogenous precursors (Seidenfaden, et al., 2006). Neuroblasts, characterized by a leading and a trailing process and the expression of TUJ1, doublecortin and PSA-NCAM (Bonfanti and Theodosis, 1994), migrate along the RMS towards the olfactory bulb (Rousselot, et al., 1995), where they further differentiate into mature NeuN$^+$ neurons. We evaluated whether ES derived *in vitro* generated neural cells have the same ability to migrate and differentiate along the RMS and whether this behavior is influenced by PSA-NCAM enrichment of *in vitro* differentiating cells. To this end, GFP$^+$ unsorted and PSA-NCAM enriched cells were transplanted in the RMS of adult mice at a long distance (around 4 mm) from the lateral ventricle, in order to reduce the influence of the SVZ neurogenic niche (Figs. 6A, H).

Ten days post grafting some GFP$^+$ cells entered the RMS, displayed the typical elongated morphology of migrating neuroblasts and were positive for PSA-NCAM and TUJ1 (Figs. 6F, 4A–D). Cells enriched for PSA-NCAM prior to grafting migrated to a much higher percentage (73.5% ± 9.1) along the RMS as compared to the unsorted control cells (5.6% ± 4.5) (Fig. 6B). We collected sequential confocal single z-stack images covering the area from the graft point at the RMS level to the OB and measured the migration distance of each GFP$^+$ cell (Fig. 6C). Cells from the unsorted population remained close to the area of the graft, mostly at a distance below 240 mm and exhibited projecting thick filaments along the RMS (Figs. 6A, D, E). In contrast, most of the PSA-NCAM enriched cells that entered the RMS were distributed over 500 mm from the graft area with some cells reaching the OB and starting to migrate radially towards the glomerular cell layer (Figs. 6F–H). However, we did not observe cells integrated in the granule cell layer or in the glomerular layer of the OB.

A different situation was observed after 40 days post grafting. At this time point the RMS was always devoid of grafted cells with migratory morphology, both in the unsorted and PSA-NCAM enriched population. Grafted cells that were still present in the RMS, had a more differentiated morphology, characterized by long and branched projections. At this time point GFP$^+$ cells were undetectable in the central OB and the different neuronal layers.

Discussion

Pluripotent stem cells (PSCs) like ESCs or induced pluripotent stem cells (iPSCs) are an attractive source for cell replacement therapy. They can be expanded and differentiated in virtually any cell type. Several studies have demonstrated the production of neuronal (Friling, et al., 2009; Lee, et al., 2000; Okabe, et al., 1996; Wichterle, et al., 2002) and glial (Brustle et al., 1999; Liu et al., 2000) lineage phenotypes from ESCs by using various techniques. Despite advances in development of different neural induction conditions for mESCs or hESCs, protocols end generally in mixed populations containing neural cells at different development stages,

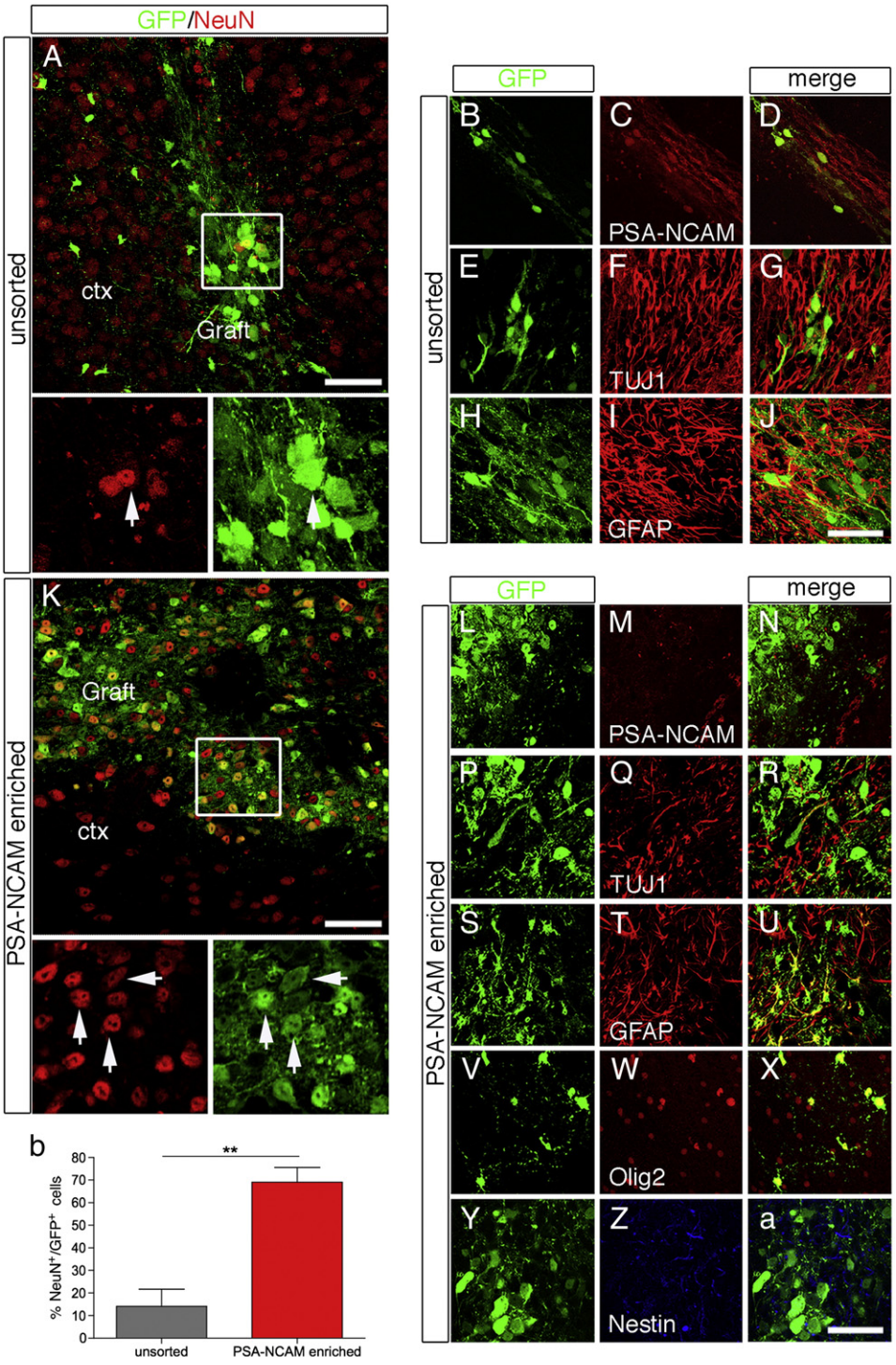

Figure 5 *In vivo* maturation of PSA-NCAM-enriched *versus* unsorted mESC derived neural precursors. (A–J) Immunofluorescence analysis of the unsorted population at 40 days post graft. Double positive cells for GFP (green), NeuN (A, red), PSA-NCAM (B–D, red), TUJ1 (E–G, red), and GFAP (H–J, red). (K–a) Immunofluorescence analysis of the PSA-NCAM enriched population (GFP^+, green) at 40 days post graft. Graft core area positive for NeuN (K, red). No GPF/PSA-NCAM (red) double-immunopositive cells are detected (L–N). Double-immunopositive cells for GFP (green), TUJ1 (P–Q, red), GFAP (S–U), and Olig2 (V–X, red). No cells are found double positive for GFP and nestin (Y–a, blue). (b) Quantification of the data presented in A, K; mean ± S.E.M., $n = 3$ (mice): $^{**}P < 0.01$. Scale bar = 50 μm. Abbreviations: GFP, green fluorescent protein; PSA-NCAM, polysialylated neural cell adhesion molecule; GFAP glial fibrillary acidic protein; Olig2, oligodendrocyte transcription factor 2; ctx, cortex. For each marker 3–4 animals were analyzed.

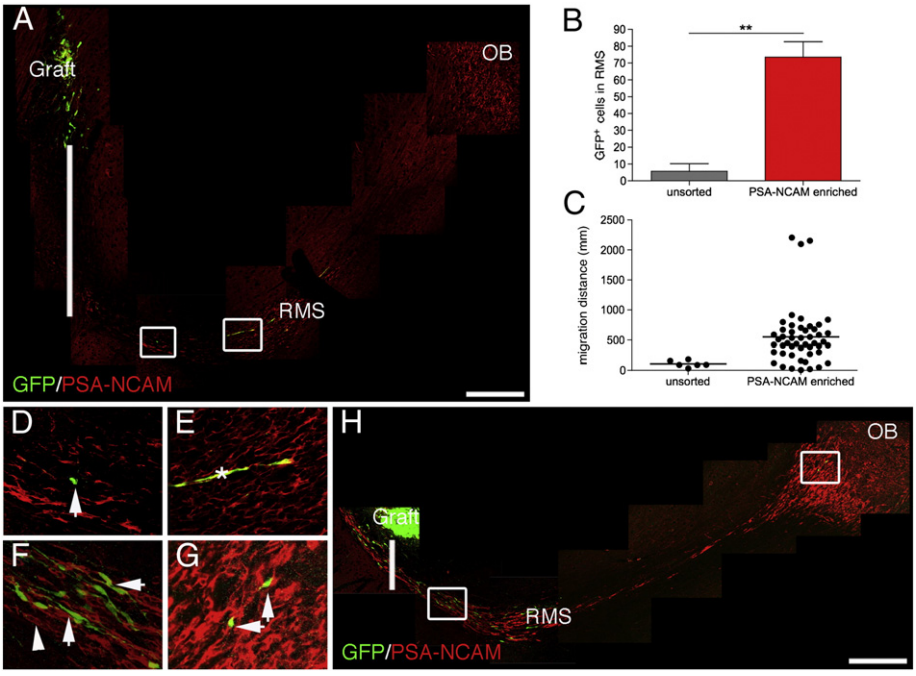

Figure 6 Migration of PSA-NCAM *in vitro* derived neural precursors. (A, H) High resolution image reconstructions covering the area from the graft point at the RMS level to the OB. Double staining for GFP (green) and PSA-NCAM (red). White bars represent the starting point for measurement of the distance length. (B) Quantification of the GFP$^+$ cells from graft level to OB; mean ± S.E.M., $n = 3$ (mice): **$P < 0.01$. (C) Migration distance covered by grafted cells in two representative animals. (D, E) Insets in A (left and right respectively) showing only few cells (arrow) and fiber extensions (asterisk) GFP$^+$/PSA-NCAM$^+$ in RMS. (F, G) Insets in H, left and right respectively, showing GFP$^+$ cells with elongated morphology integrated in the RMS host structure (F, arrows) and GFP$^+$ cells at the entrance of OB. Scale bar = 200 μm (A, H); 20 μm (D–G). Abbreviations: GFP, green fluorescent protein; PSA-NCAM, polysialylated neural cell adhesion molecule; RMS, rostral migratory stream; OB olfactory bulb.

undifferentiated ESCs and cells of non-neural identity. The use of flow cytometry or magnetic sorting techniques based on specific neural cell surface markers has been suggested to improve *in vitro* differentiation protocols by simply enriching desired cell or depleting unwanted ones (Bosio, et al., 2009; Pruszak, et al., 2007). In view of a translational approach where eventually a clinical grade, gentle and fast isolation of cells needs to be performed we decided to choose magnetic cell sorting (MACS) as the sorting technology (Bosio, et al., 2009). Most of the sorting strategies applied until now required transgenic techniques (Hedlund et al., 2007, 2008; Xian, et al., 2003) or the combination of two or more different surface markers (Cremer, et al., 1998; Pruszak, et al., 2009, 2007; Yuan, et al., 2011). We decided to develop a simple strategy for purification of neuronal precursors based on a single precursor marker. The choice of the neural subpopulation to be enriched has proved challenging. Previous studies on human ESCs reported that despite enrichment of specific subpopulations of neurons, grafts exhibited expanding clusters of undifferentiated mitotic neuroepithelial cells, which can be tumorigenic (Roy, et al., 2006). Moreover, cells too advanced in their differentiation failed to survive in the host tissue, showing poor engraftment by evidence of inflammation and dead cells (MacLaren, et al., 2006). We focused our attention on a specific subpopulation of neural precursors that is characterized by the expression of the extracellular PSA modification. During embryonic development virtually all the future mature neurons express PSA-NCAM and previous studies demonstrated that neural precursors derived from NTera2 cells and enriched for PSA-NCAM were able to further differentiate in specific subpopulation *in vitro* (Schwartz et al., 2005). In our study we demonstrated that PSA-NCAM was also differentially expressed during *in vitro* differentiation of mESCs and developed a protocol for magnetic enrichment of ES derived PSA-NCAM$^+$ cells. PSA-NCAM *in vitro* derived positive cells were found to have neural feature based on the upregulation of several genes involved in neuronal development and characteristic of neural precursors. Moreover, following *in vitro* neuronal differentiation, PSA-NCAM$^+$ cells efficiently generated neurons as demonstrated by the increased number of TUJ1, MAP2 and GAD67 positive cells and the up-regulation of several neuronal genes compared to control cells where no enrichment was applied. Enrichment for PSA-NCAM not only increased the neuronal differentiation potential of the protocol applied here, but also robustly removed teratoma-forming pluripotent stem cells as demonstrated both by the dramatic decrease of Oct4 positive cells and the down-regulation of genes involved in maintenance of pluripotency. However, according to staining with the cell cycle marker Ki67, no significant reduction of proliferative cells was detected after differentiation of the PSA-NCAM-enriched neural precursors. Our observation of proliferative cells derived from PSA-NCAM enriched cells can either be explained by contaminants or by the point that PSA-NCAM$^+$ cells themselves can be proliferative. Given the high degree of purity we achieved we favor the hypothesis that the ES derived PSA-NCAM$^+$ cells have a rather embryonic, proliferative phenotype.

Beyond the finding that PSA-NCAM enrichment could be useful to improve the *in vitro* neuronal differentiation protocol, we also addressed the question whether PSA-NCAM-expressing neural progenitors are a potential source for cell replacement therapies. In a previous study, enrichment of PSA-NCAM$^+$-precursors was applied previous transplantation with unsatisfactory results due to a low number of surviving neurons (Friling, et al., 2009). Here we demonstrate that magnetically enriched PSA-NCAM$^+$ precursors not only survived well in the host tissue, but also increased the number of mature neurons *in vivo*. Moreover, PSA-NCAM$^+$-ES cell-derived precursors did not fail to migrate when grafted in a responsive anatomical area like the RMS. The influence of the PSA modification on the migration of cells in embryonic and adult neurogenic areas has been known for a while (for review see Bonfanti, 2006; Durbec and Cremer, 2001). Overexpression of PSA-NCAM in ES cell-derived glial precursors strikingly modified their migration behavior in response to guidance cues as demonstrated by chemotaxis assays and *in vivo* studies (Glaser et al., 2007). We demonstrate here that mESC derived cells endogenously expressing PSA-NCAM respond to *in vivo* cues. Tabar et al. reported that human ES cell derived neural precursors that where grafted in the SVZ and displayed the ability to migrate and to further differentiate (Tabar et al., 2005). However, when cells are grafted into the SVZ their further behavior might be imposed by the strong neurogenic environment and does not directly reflect their intrinsic program. Therefore, in our study, to better assess migration and differentiation ability, PSA-NCAM$^+$ cells where grafted directly in the RMS, distant to the SVZ niche. This might explain why in our study cells failed to become GABAergic and dopaminergic interneurons in the granular and glomerular layers of the OB.

The origin of the glial cells seen both *in vitro* and *in vivo* needs to be analyzed further. The Olig2 and GFAP-immunopositive cells might develop from contaminants present in the positive fraction after sorting and increase their frequency in the final population due to their higher proliferation rate. On the other hand, glial cells might differentiate from the PSA-NCAM expressing cells. Indeed, unlike its prevalent distribution in cells of the neuronal lineage within the mature nervous tissue, PSA-NCAM is also associated with glial precursors during development (for review see Bonfanti, 2006). For example, a previous study demonstrated *in vitro* that among PSA-NCAM$^+$ cells isolated from neonatal brain were oligondendrocyte pre-progenitors, corresponding to early precursors of the oligondendrocyte-type2 astrocyte (O-2A) lineage (Ben-Hur, et al., 1998). Moreover, PSA-NCAM$^+$ cell precursors used for transplantation in a focal demyelinating lesion were found to produce remyelinating Schwann cells in the CNS (Keirstead et al., 1999).

It remains to be investigated if enrichment for PSA-NCAM expressing neural precursors from ES derived cells could also help to better restore lost function in animal disease models and whether the findings with mouse cells can be translated to human cells. Good promises in this direction come from a recent study where PSA-NCAM enrichment was applied to improve purity during *in vitro* neural differentiation protocol of hESCs (Mak et al., 2012). Furthermore, the tumorigenic potential of the enriched population has to be addressed in greater detail. Here we show promising results based on a decreased number of Oct4 expressing cells and missing abnormal cell growth in the *in vivo* studies. However, it has to be noticed that an extended proliferation level was observed both *in vitro* and *in vivo* after short time points post sorting albeit not after 40 days. Therefore, we cannot exclude the risk of tumor formation, especially after longer time periods than studied here.

In summary, PSA-NCAM based-lineage selection permits efficient enrichment of young ES cell-derived neuronal precursors, relying on a single endogenous marker and avoiding genetic modification. If this general strategy can be translated to human cells it might represent a preferred strategy for exploring future therapeutic applications.

Supplementary data to this article can be found online at http://dx.doi.org/10.1016/j.scr.2012.10.005.

Author disclosure statement

Josephine Ecklebe, Stefan Tomiuk, Dominik Eckardt and Andreas Bosio are all employees at Miltenyi Biotech GmbH. Serena Barral was granted a Marie Curie post-doc at Miltenyi Biotec GmbH and subsequently post-doc for Miltenyi Biotec GmbH during the preparation of this scientific work. For Marie-Catherine Tiveron and Harold Cremer no competing financial interests exist.

Acknowledgment

Sabine Peiffer and Silvia Rüberg at Miltenyi Biotec GmbH are thanked for their coordination of the microarray data generation. Christophe Beclin is thanked for his help in manuscript revision. The authors acknowledge the European Union for funding through Marie Curie research training network AXREGEN and IAPP DopaNew. HC is supported by grants from the Agence National de la Recherche (ForDopa), Fondation pour la Récherche Médicale (Equipe FRM) and the Fondation de France.

References

Angata, K., Fukuda, M., 2003. Polysialyltransferases: major players in polysialic acid synthesis on the neural cell adhesion molecule. Biochimie 85 (1–2), 195–206.

Ben-Hur, T., Rogister, B., Murray, K., Rougon, G., Dubois-Dalcq, M., 1998. Growth and fate of PSA-NCAM+ precursors of the postnatal brain. J. Neurosci. 18 (15), 5777–5788.

Bjorklund, L.M., Sanchez-Pernaute, R., Chung, S., Andersson, T., Chen, I.Y., McNaught, K.S., Isacson, O., 2002. Embryonic stem cells develop into functional dopaminergic neurons after transplantation in a Parkinson rat model. Proc. Natl. Acad. Sci. U. S. A. 99 (4), 2344–2349.

Bonfanti, L., 2006. PSA-NCAM in mammalian structural plasticity and neurogenesis. Prog. Neurobiol. 80 (3), 129–164.

Bonfanti, L., Theodosis, D.T., 1994. Expression of polysialylated neural cell adhesion molecule by proliferating cells in the subependymal layer of the adult rat, in its rostral extension and in the olfactory bulb. Neuroscience 62 (1), 291–305.

Bonfanti, L., Merighi, A., Theodosis, D.T., 1996. Dorsal rhizotomy induces transient expression of the highly sialylated isoform of the neural cell adhesion molecule in neurons and astrocytes of the adult rat spinal cord. Neuroscience 74 (3), 619–623.

Bosio, A., Huppert, V., Donath, S., Hennemann, P., Malchow, M., Heinlein, U.A., 2009. Isolation and enrichment of stem cells. Adv. Biochem. Eng. Biotechnol. 114, 23–72.

Brustle, O., Jones, K.N., Learish, R.D., Karram, K., Choudhary, K., Wiestler, O.D., McKay, R.D., 1999. Embryonic stem cell-derived glial precursors: a source of myelinating transplants. Science 285 (5428), 754–756.

Chung, S., Sonntag, K.C., Andersson, T., Bjorklund, L.M., Park, J.J., Kim, D.W., Kim, K.S., 2002. Genetic engineering of mouse embryonic stem cells by Nurr1 enhances differentiation and maturation into dopaminergic neurons. Eur. J. Neurosci. 16 (10), 1829–1838.

Chung, S., Moon, J.I., Leung, A., Aldrich, D., Lukianov, S., Kitayama, Y., Kim, K.S., 2011. ES cell-derived renewable and functional midbrain dopaminergic progenitors. Proc. Natl. Acad. Sci. U. S. A. (23), 9703–9708.

Cremer, H., Lange, R., Christoph, A., Plomann, M., Vopper, G., Roes, J., et al., 1994. Inactivation of the N-CAM gene in mice results in size reduction of the olfactory bulb and deficits in spatial learning. Nature 367 (6462), 455–459.

Cremer, H., Chazal, G., Carleton, A., Goridis, C., Vincent, J.D., Lledo, P.M., 1998. Long-term but not short-term plasticity at mossy fiber synapses is impaired in neural cell adhesion molecule-deficient mice. Proc. Natl. Acad. Sci. U. S. A. 95 (22), 13242–13247.

Durbec, P., Cremer, H., 2001. Revisiting the function of PSA-NCAM in the nervous system. Mol. Neurobiol. 24 (1–3), 53–64.

Duveau, V., Arthaud, S., Rougier, A., Le Gal La Salle, G., 2007. Polysialylation of NCAM is upregulated by hyperthermia and participates in heat shock preconditioning-induced neuroprotection. Neurobiol. Dis. 26 (2), 385–395.

El Maarouf, A., Rutishauser, U., 2003. Removal of polysialic acid induces aberrant pathways, synaptic vesicle distribution, and terminal arborization of retinotectal axons. J. Comp. Neurol. 460 (2), 203–211.

El Maarouf, A., Petridis, A.K., Rutishauser, U., 2006. Use of polysialic acid in repair of the central nervous system. Proc. Natl. Acad. Sci. U. S. A. 103 (45), 16989–16994.

Finne, J., 1982. Occurrence of unique polysialosyl carbohydrate units in glycoproteins of developing brain. J. Biol. Chem. 257 (20), 11966–11970.

Finne, J., Finne, U., Deagostini-Bazin, H., Goridis, C., 1983. Occurrence of alpha 2–8 linked polysialosyl units in a neural cell adhesion molecule. Biochem. Biophys. Res. Commun. 112 (2), 482–487.

Franz, C.K., Rutishauser, U., Rafuse, V.F., 2005. Polysialylated neural cell adhesion molecule is necessary for selective targeting of regenerating motor neurons. J. Neurosci. 25 (8), 2081–2091.

Friling, S., Andersson, E., Thompson, L.H., Jonsson, M.E., Hebsgaard, J.B., Nanou, E., Ericson, J., 2009. Efficient production of mesencephalic dopamine neurons by Lmx1a expression in embryonic stem cells. Proc. Natl. Acad. Sci. U. S. A. 106 (18), 7613–7618.

Glaser, T., Brose, C., Franceschini, I., Hamann, K., Smorodchenko, A., Zipp, F., Brustle, O., 2007. Neural cell adhesion molecule polysialylation enhances the sensitivity of embryonic stem cell-derived neural precursors to migration guidance cues. Stem Cells 25 (12), 3016–3025.

Golebiewska, A., Atkinson, S.P., Lako, M., Armstrong, L., 2009. Epigenetic landscaping during hESC differentiation to neural cells. Stem Cells 27 (6), 1298–1308.

Hadjantonakis, A.K., Gertsenstein, M., Ikawa, M., Okabe, M., Nagy, A., 1998. Generating green fluorescent mice by germline transmission of green fluorescent ES cells. Mech. Dev. 76 (1–2), 79–90.

Hedlund, E., Pruszak, J., Ferree, A., Vinuela, A., Hong, S., Isacson, O., Kim, K.S., 2007. Selection of embryonic stem cell-derived enhanced green fluorescent protein-positive dopamine neurons using the tyrosine hydroxylase promoter is confounded by reporter gene expression in immature cell populations. Stem Cells 25 (5), 1126–1135.

Hedlund, E., Pruszak, J., Lardaro, T., Ludwig, W., Vinuela, A., Kim, K.S., Isacson, O., 2008. Embryonic stem cell-derived Pitx3-enhanced green fluorescent protein midbrain dopamine neurons survive enrichment by fluorescence-activated cell sorting and function in an animal model of Parkinson's disease. Stem Cells 26 (6), 1526–1536.

Karaca, M., Castel, J., Tourrel-Cuzin, C., Brun, M., Geant, A., Dubois, M., Ctesson, S., Rodriguez, M., Luquet, S., Cattan, P., Lockhart, B., Lang, J., Ktorza, A., Magnan, C., Kargar, C., 2009. Exploring functional beta-cell heterogeneity in vivo using PSA-NCAM as a specific marker. PLoS One 4 (5), e5555.

Kawasaki, H., Mizuseki, K., Nishikawa, S., Kaneko, S., Kuwana, Y., Nakanishi, S., Sasai, Y., 2000. Induction of midbrain dopaminergic neurons from ES cells by stromal cell-derived inducing activity. Neuron 28 (1), 31–40.

Keirstead, H.S., Ben-Hur, T., Rogister, B., O'Leary, M.T., Dubois-Dalcq, M., Blakemore, W.F., 1999. Polysialylated neural cell adhesion molecule-positive CNS precursors generate both oligodendrocytes and Schwann cells to remyelinate the CNS after transplantation. J. Neurosci. 19 (17), 7529–7536.

Kiss, J.Z., Rougon, G., 1997. Cell biology of polysialic acid. Curr. Opin. Neurobiol. 7 (5), 640–646.

Lee, S.H., Lumelsky, N., Studer, L., Auerbach, J.M., McKay, R.D., 2000. Efficient generation of midbrain and hindbrain neurons from mouse embryonic stem cells. Nat. Biotechnol. 18 (6), 675–679.

Liu, S., Qu, Y., Stewart, T.J., Howard, M.J., Chakrabortty, S., Holekamp, T.F., McDonald, J.W., 2000. Embryonic stem cells differentiate into oligodendrocytes and myelinate in culture and after spinal cord transplantation. Proc. Natl. Acad. Sci. U. S. A. 97 (11), 6126–6131.

MacLaren, R.E., Pearson, R.A., MacNeil, A., Douglas, R.H., Salt, T.E., Akimoto, M., Ali, R.R., 2006. Retinal repair by transplantation of photoreceptor precursors. Nature 444 (7116), 203–207.

Mak, S.K., Huang, Y.A., Iranmanesh, S., Vangipuram, M., Sundararajan, R., Nguyen, L., Langston, J.W., Schüle, B., 2012. Small molecules greatly improve conversion of human-induced pluripotent stem cells to the neuronal lineage. Stem Cells Int. 140427.

Martinat, C., Bacci, J.J., Leete, T., Kim, J., Vanti, W.B., Newman, A.H., Abeliovich, A., 2006. Cooperative transcription activation by Nurr1 and Pitx3 induces embryonic stem cell maturation to the midbrain dopamine neuron phenotype. Proc. Natl. Acad. Sci. U. S. A. 103 (8), 2874–2879.

Muller, D., Wang, C., Skibo, G., Toni, N., Cremer, H., Calaora, V., Kiss, J.Z., 1996. PSA-NCAM is required for activity-induced synaptic plasticity. Neuron 17 (3), 413–422.

Nguyen, L., Rigo, J.M., Malgrange, B., Moonen, G., Belachew, S., 2003. Untangling the functional potential of PSA-NCAM-expressing cells in CNS development and brain repair strategies. Curr. Med. Chem. 10 (20), 2185–2196.

Okabe, S., Forsberg-Nilsson, K., Spiro, A.C., Segal, M., McKay, R.D., 1996. Development of neuronal precursor cells and functional postmitotic neurons from embryonic stem cells in vitro. Mech. Dev. 59 (1), 89–102.

Pham, K., Nacher, J., Hof, P.R., McEwen, B.S., 2003. Repeated restraint stress suppresses neurogenesis and induces biphasic PSA-NCAM expression in the adult rat dentate gyrus. Eur. J. Neurosci. 17 (4), 879–886.

Pruszak, J., Sonntag, K.C., Aung, M.H., Sanchez-Pernaute, R., Isacson, O., 2007. Markers and methods for cell sorting of human embryonic stem cell-derived neural cell populations. Stem Cells 25 (9), 2257–2268.

Pruszak, J., Ludwig, W., Blak, A., Alavian, K., Isacson, O., 2009. CD15, CD24, and CD29 define a surface biomarker code for neural lineage differentiation of stem cells. Stem Cells 27 (12), 2928–2940.

Rousselot, P., Lois, C., Alvarez-Buylla, A., 1995. Embryonic (PSA) N-CAM reveals chains of migrating neuroblasts between the lateral ventricle and the olfactory bulb of adult mice. J. Comp. Neurol. 351 (1), 51–61.

Roy, N.S., Cleren, C., Singh, S.K., Yang, L., Beal, M.F., Goldman, S.A., 2006. Functional engraftment of human ES cell-derived dopaminergic neurons enriched by coculture with telomerase-immortalized midbrain astrocytes. Nat. Med. 12 (11), 1259–1268.

Rutishauser, U., Landmesser, L., 1996. Polysialic acid in the vertebrate nervous system: a promoter of plasticity in cell–cell interactions. Trends Neurosci. 19 (10), 422–427.

Schwartz, C.M., Spivak, C.E., Baker, S.C., McDaniel, T.K., Loring, J.F., Nguyen, C., Rao, M.S., 2005. NTera2: a model system to study dopaminergic differentiation of human embryonic stem cells. Stem Cells Dev. 14 (5), 517–534.

Seidenfaden, R., Desoeuvre, A., Bosio, A., Virard, I., Cremer, H., 2006. Glial conversion of SVZ-derived committed neuronal precursors after ectopic grafting into the adult brain. Mol. Cell. Neurosci. 32 (1–2), 187–198.

Sharp, J., Keirstead, H.S., 2009. Stem cell-based cell replacement strategies for the central nervous system. Neurosci. Lett. 456 (3), 107–111.

Tabar, V., Panagiotakos, G., Greenberg, E.D., Chan, B.K., Sadelain, M., Gutin, P.H., Studer, L., 2005. Migration and differentiation of neural precursors derived from human embryonic stem cells in the rat brain. Nat. Biotechnol. 23 (5), 601–606.

Thomson, J.A., Itskovitz-Eldor, J., Shapiro, S.S., Waknitz, M.A., Swiergiel, J.J., Marshall, V.S., Jones, J.M., 1998. Embryonic stem cell lines derived from human blastocysts. Science 282 (5391), 1145–1147.

Tropepe, V., Hitoshi, S., Sirard, C., Mak, T.W., Rossant, J., van der Kooy, D., 2001. Direct neural fate specification from embryonic stem cells: a primitive mammalian neural stem cell stage acquired through a default mechanism. Neuron 30 (1), 65–78.

Wichterle, H., Lieberam, I., Porter, J.A., Jessell, T.M., 2002. Directed differentiation of embryonic stem cells into motor neurons. Cell 110 (3), 385–397.

Xian, H.Q., McNichols, E., St Clair, A., Gottlieb, D.I., 2003. A subset of ES-cell-derived neural cells marked by gene targeting. Stem Cells 21 (1), 41–49.

Ying, Q.L., Stavridis, M., Griffiths, D., Li, M., Smith, A., 2003. Conversion of embryonic stem cells into neuroectodermal precursors in adherent monoculture. Nat. Biotechnol. 21 (2), 183–186.

Yuan, S.H., Martin, J., Elia, J., Flippin, J., Paramban, R.I., Hefferan, M.P., Carson, C.T., 2011. Cell-surface marker signatures for the isolation of neural stem cells, glia and neurons derived from human pluripotent stem cells. PLoS One 6 (3), e17540.